

A mineralogical record of ocean change: Decadal and centennial patterns in the California mussel

Sophie J. McCoy¹  | Nicholas A. Kamenos²  | Peter Chung² |
Timothy J. Wootton³  | Catherine A. Pfister³ 

¹Department of Biological Science, Florida State University, Tallahassee, FL, USA

²School of Geographical and Earth Science, University of Glasgow, Glasgow, Scotland

³Department of Ecology and Evolution, University of Chicago, Chicago, IL, USA

Correspondence

Sophie J. McCoy, Department of Biological Science, Florida State University, Tallahassee, FL, USA.
Email: mccoy@bio.fsu.edu

Funding information

Marine Alliance for Science and Technology Scotland (MASTS); European Commission 7th Research Framework Programme (FP7), Grant/Award Number: 330271; The SeaDoc Society, Grant/Award Number: NSF grants OCE01-17801, OCE09-28232, DEB09-19420, DEB15-56874

Abstract

Ocean acidification, a product of increasing atmospheric carbon dioxide, may already have affected calcified organisms in the coastal zone, such as bivalves and other shellfish. Understanding species' responses to climate change requires the context of long-term dynamics. This can be particularly difficult given the longevity of many important species in contrast with the relatively rapid onset of environmental changes. Here, we present a unique archival dataset of mussel shells from a locale with recent environmental monitoring and historical climate reconstructions. We compare shell structure and composition in modern mussels, mussels from the 1970s, and mussel shells dating back to 1000–2420 years BP. Shell mineralogy has changed dramatically over the past 15 years, despite evidence for consistent mineral structure in the California mussel, *Mytilus californianus*, over the prior 2500 years. We present evidence for increased disorder in the calcium carbonate shells of mussels and greater variability between individuals. These changes in the last decade contrast markedly from a background of consistent shell mineralogy for centuries. Our results use an archival record of natural specimens to provide centennial-scale context for altered mineralogy and variability in shell features as a response to acidification stress and illustrate the utility of long-term studies and archival records in global change ecology. Increased variability between individuals is an emerging pattern in climate change responses, which may equally expose the vulnerability of organisms and the potential of populations for resilience.

KEYWORDS

calcium carbonate, crystallography, electron backscatter diffraction, mineralogy, mussels, *Mytilus*, ocean acidification, Raman spectroscopy

1 | INTRODUCTION

Current uncertainty regarding organismal responses to ongoing climate changes deals with the juxtaposed issues of scale and mechanism: laboratory studies enable the isolation of a specific stressor, while field studies are necessary to truly understand effects of a stressor in a natural, often more variable, system. While field studies also can detect long-term evolutionary or population dynamics (Hofmann et al., 2010; Pfister et al., 2016), the length of time required to see a

response can be prohibitive. Organisms that retain growth history records over millennial timescales and that are relevant to contemporary environmental stressors offer a model to overcome the challenge of long-term ecological relevance (Cobb, Charles, Cheng, & Edwards, 2003; Halfar, Adey, & Kronz, 2013; Mann et al., 2008).

Calcified organisms such as bivalves are predicted to face the greatest challenges under future ocean acidification (Cooley & Doney, 2009). Some coastal areas have already experienced large changes in mean seawater acidity, in some cases equal to or greater

than conditions originally predicted in future ocean scenarios (Chan et al., 2017; Hofmann et al., 2011; Kroeker et al., 2016; Wahl et al., 2015; Wootton & Pfister, 2012; Wootton, Pfister, & Forester, 2008). For example, seawater pH has declined rapidly in the northeast Pacific over the last 17 years, accompanied by changes in $\delta^{13}\text{C}$ signatures from mussel shells, which reveal altered inorganic carbon chemistry over recent decades (Pfister et al., 2011).

Calcification can be affected by multiple environmental parameters, including pCO_2 (Fitzer, Cusack, Phoenix, & Kamenos, 2014; Gazeau et al., 2013; Kroeker, Kordas, Crim, & Singh, 2010; Pfister et al., 2016), temperature (Fitzer et al., 2015), wave exposure (Fox & Coe, 1943), food availability (Coe, 1945; Hahn et al., 2011; Thomsen & Melzner, 2010; Waldbusser et al., 2013), predation pressure (Vermeij, 1976), and their interacting effects (Kroeker, Kordas, & Harley, 2017; Melzner et al., 2011). These calcification responses include changes in growth rate and overall size (Thomsen & Melzner, 2010), changes in shell morphology (Fitzer et al., 2015; Pfister et al., 2016), and mineralogical plasticity (Nash et al., 2012; Pauly, Kamenos, Donohue, & LeDrew, 2015). Mineralogical plasticity has been proposed as a potentially beneficial adaptive mechanism (Fitzer et al., 2014; Leung, Russell, & Connell, 2017) that allows calcified organisms to continue growth under acidified conditions. However, ecological and physiological trade-offs exist between mineralogy, morphology, and mineral strength that can lead to ecological repercussions of environmentally induced skeletal changes (McCoy & Pfister, 2014; McCoy & Ragazzola, 2014), and changes in mussel shell shape or thickness may be detrimental to their survival in natural conditions (Fitzer et al., 2015; Gooding, Harley, & Tang, 2009; Pfister et al., 2016). Laboratory studies have shown mineralogical changes to occur over relatively short timescales (<6 months) in both adults and juveniles (Fitzer et al., 2014, 2016; Melzner et al., 2011) and to be especially important to larval and other early developmental stages (Stumpp, Wren, Melzner, Thorndyke, & Dupont, 2011; Thomsen, Haynert, Wegner, & Melzner, 2015; Waldbusser et al., 2013).

While specific calcification mechanisms in bivalves remain definitively unknown (Thomsen et al., 2015), amorphous calcium carbonate, which lacks clear crystallographic structure, has been suggested as a precursor to calcium carbonate crystals. Amorphous calcium carbonate is produced within an intracellular compartment and transported to the site of calcification (Mount, Wheeler, Paradkar, & Snider, 2004; Weiner & Addadi, 2011), where it can either remain amorphous or crystallize into aragonite or calcite as dictated by the presence of matrix proteins (Jacob et al., 2008; Weiss, Tuross, Addadi, & Weiner, 2002). The production of costly matrix proteins necessary to complete the calcification process may be reduced under stress, resulting in longer persistence of amorphous calcium carbonate (Fitzer et al., 2016; Palmer, 1983).

Whether an organism produces aragonite or calcite may also reflect local conditions. Aragonite is more soluble than the calcite polymorph of calcium carbonate, and therefore at greater risk of dissolution from elevated pCO_2 (Feely et al., 2012). Under ocean-wide ocean-acidification conditions predicted to occur by 2001, saturation of aragonite in the surface ocean will decline faster than that of calcite

and cause dissolution of aragonitic shells, such as those of planktonic pteropods (Orr et al., 2005) and benthic corals and mollusks (Hall-Spencer et al., 2008). Seawater magnesium concentrations may also mediate how calcium carbonate structures are made (Ries, 2005). Thermodynamically, aragonite or high-Mg calcite precipitation is favored when seawater concentrations of Mg are elevated, and calcite precipitation is favored when seawater Mg concentrations are low (Ries, Anderson, & Hill, 2008). A similar mechanism was documented in typically high-Mg calcite coralline algae, which were more resistant to ocean acidification when their skeletons included the stable Mg-bearing carbonate dolomite (Nash et al., 2012). Thus, crystal phase, crystal structure, and carbonate Mg content are all potential causes of mineralogical variation in response to ocean acidification. Possible responses include those that may be beneficial to organisms in the long-term, such as mineralogical shifts to more stable carbonate polymorphs. However, other responses may be driven by short-term energetic effects that will result in weaker or more soluble shells, perhaps conversely to short-term ecological forces, such as predation.

The California mussel, *Mytilus californianus*, ranges from Alaska to Baja California along the coastline of the eastern Pacific Ocean, which experiences seasonal upwelling of acid seawater (Feely, Sabine, Hernandez-Ayon, Ianson, & Hales, 2008). *Mytilus californianus* lays down an additional region of inner prismatic calcite, a shell layer which is unique to *M. californianus* among mussel species worldwide (Dodd, 1964). This trait may have evolved in response to long-term local acidification via upwelling in the California Current System to protect the aragonitic nacreous layer, and it is present in our midden shell samples dating back to AD 663. Regardless of its origin, it will likely be advantageous to *M. californianus* as ocean pH declines and its surroundings become more corrosive.

Previous work has shown that the thickness of annual growth bands within the inner prismatic layer of *M. californianus* is reduced by approximately half when comparing modern day specimens to shells dated to 1000–1340 years BP at Tatoosh Island, WA (Pfister et al., 2016), suggesting that modern shells may be experiencing stress associated with biomineralization through time. Here, we present a study of shell structure from the California mussel, *M. californianus*, spanning decadal and centennial scales to determine the long-term effects of changes in ocean carbon chemistry on shell mineralogy in a natural system. Alterations to modern shells that would be expected if calcification is increasingly stressful or costly may include: a changed crystal structure, increases in the less soluble calcite polymorph, and increased Mg content in the CaCO_3 lattice. Reduced mineral organization was interpreted as a possible effect of increased energy load of biomineralization, while increased variability between shells within a time period suggests environmental stress.

2 | MATERIALS AND METHODS

2.1 | Sample collection and preparation

Mytilus californianus were collected live from Tatoosh Island, WA (48.32°N, 127.74°W) in spring of 2009, 2011, and 2015 at two

sites, N- and SW-facing, on the island. Adult *M. californianus* from two locations at Sand Point (48.126°N, 124.702°W), Sand Point North and Yellow Banks, were collected in July and August 2010. These collections comprise the 'modern' sampling effort. 'Archival' shells were collected live from Tatoosh Island in the 1970s by T. Suchanek from a SW-facing region of the island. Excavation of Native American middens from the Makah Tribe (McMillan, 2000), who used Tatoosh Island as a summer camp prior to the 1800s and historically had a large settlement at Sand Point, provided 'midden' valves from Tatoosh Island through the Makah Cultural and Resource Center, while Sand Point midden material was provided by the Olympic National Park. These shells were radiocarbon dated using shell material from their most recent year of growth, with Tatoosh Island midden shells dated to 1000–1340 years BP in 2010 (Pfister et al., 2011) and Sand Point midden shells dated to 2150–2440 years BP in 2015 (Pfister et al., 2016). Valves were cross-sectioned along their axis of maximum growth using a slow-speed saw with a diamond blade to make a 3 mm-thick cross-section. Cross-sections were mounted on glass slides and polished on 800–4,000 grit silicon carbide paper, followed by aluminum oxide (0.3 and 1 μm) and colloidal silica (0.6 μm) suspensions. Cross-sections were scanned at high resolution prior to analysis to provide a sample image map.

2.2 | EBSD imaging

Electron backscatter diffraction (EBSD) was performed to image the crystallographic orientation of shell calcite. A 20 kV beam voltage was utilized under low vacuum mode (~ 50 Pa) on an FEI Quanta 200 F Environmental SEM (University of Glasgow, School of Geographical and Earth Science), with a stage tilt of 70° to detect backscatter Kikuchi patterns (Pérez-Huerta et al., 2009). Scans were conducted within the inner prismatic layer of *M. californianus*, well outside of the beak area (Dodd, 1964) Figure S1. In shells HC09006 (modern, collected live in 2009) and TI09001 (midden, radiocarbon aged to 1170 yBP), full transects were imaged from the outermost (oldest shell growth) to the innermost (youngest) calcite bands at 0.5 μm resolution. In shells HC15003, HC15004, GL15005, GL15007 (modern, 2015), GL09002 (modern, 2009), TS10002, TS10004 (archival, 1975), TI09001 (midden, 1170 yBP), TI09004 (midden, 1100 yBP), TI09007 (midden, 1060 yBP) and TI09008 (midden, 1050 BP), a section containing one full summer and winter growth cycle from the middle of the shell (to avoid possible age effects from young or elderly growth layers) was imaged at 1.1 μm resolution. Crystallographic orientation maps were produced using OIM Analysis software v. 7.

2.3 | Raman spectroscopy

Transects were taken from the outermost (oldest) to innermost (youngest) calcite bands in all shells from Tatoosh Island (modern, $n = 15$; archival, $n = 5$, midden, $n = 7$) and Sand Point (modern, $n = 10$; midden, $n = 8$). Points were chosen manually at 20 \times

magnification. Replication of 3–4 \times within a growth band was taken at random across samples to test within-sample variability. Raman spectra were taken using the 785 nm near-infrared laser. Acquisition time was set to 1.00 s at 100% laser power for 10 \times accumulations per sample point (Pauly et al., 2015). Peaks were identified manually and fit using WIRE software v. 4.2. Analyses were conducted on all samples from all shells pooled. Mg-O bond strength was determined from the full width at half peak maximum (FWHM) of the Raman shift peak centered at ~ 1089 cm^{-1} and relative Mg concentrations were determined from the exact position of the peak (Bischoff, Sharma, & MacKenzie, 1985; Pauly et al., 2015).

3 | RESULTS

3.1 | Crystallographic orientation

Electron backscatter diffraction (EBSD) provides a qualitative measure of crystallographic orientation. Comparison of *M. californianus* shell growth from 1050 to 1170 AD (midden), the 1970s (archival), 2000s (modern) and 2010s (modern) revealed visually apparent changes in crystal orientation and crystal size among shell material deposited in the 2010s compared with all other time intervals (Figures 1–4). Shells from 1050 to 1170 AD show visual signs of fragility and light wear, likely from the degradation of the organic matrix that sheaths the calcium carbonate crystals during their ~ 1000 years spent in middens. However, these midden shells provide a clear record of calcite crystal organization and uniformity of crystal orientation, as does shell material deposited in the 1970s and 2000s (Figures 1–3). Shell material from the 2010s (collected in 2015) documents mosaic patterns of crystal orientation, greater disorder among crystals, smaller crystal sizes, and possible regions of disorganized or recrystallized calcium carbonate (Figure 4). We also observed greater variation in crystal orientation and size between shells in these most recent samples (Figure 4).

3.2 | Shell composition and bond strength

The low frequency vibrations detected by Raman spectroscopy indicate the elemental composition and types of bonds present in solid materials. Mg is present as a trace element in all natural marine carbonates. The Raman vibrational peak at ~ 1089 cm^{-1} has been identified as an Mg-O bond and its location is one of the peaks used to differentiate calcite and aragonite (Bischoff et al., 1985). Full width at half peak maximum (FWHM) is related to the strength of the Mg-O bond, while Raman shift of the ~ 1089 cm^{-1} peak is a proxy of Mg content of calcite (Pauly et al., 2015).

Pooled between sites, Tatoosh Island, WA and nearby Sand Point, WA on the mainland, there was a poor relationship between increases in FWHM and Raman shift on a per sample basis ($a = 0.858$, $r^2 = .238$, $p = .405$; Figure 5a). Mean FWHM increased over time from midden to modern samples from 4.3 to 4.6 (7%) at Tatoosh Island, and from 4.5 to 4.6 at Sand Point (2%) (t -test on

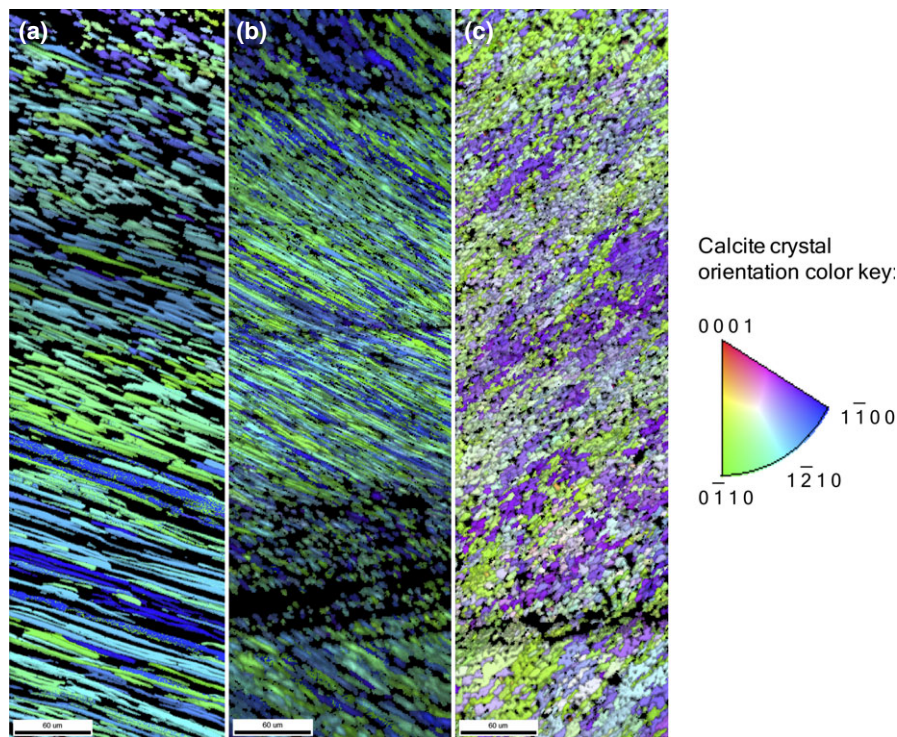


FIGURE 1 Electron backscatter diffraction (EBSD) analysis of midden mussel shells from 1060 to 1170 AD showing calcite crystallographic orientation map in reference to the {0001} plane, according to color key. Electron backscatter diffraction (EBSD) scans centered on a summer growth band from the center of the shell record (middle-age of individual), with most recent shell material at the bottom. Winter bands identified by horizontal bands of condensed crystal sizes and higher relative concentration of organic matter, revealed by black areas in the absence of crystal backscatter. (a) Shell TI09001, aged 1170 yBP, scale bar 60 μm ; (b) Shell TI09004, aged 1100 yBP, scale bar 60 μm ; (c) Shell TI09007, aged 1060 yBP, scale bar 60 μm . Refer to Figure S2 for an illustration of crystal orientation. Figure S3 shows a full transect of shell TI09001. Figure S4 shows additional scans of shell TI09007. These scans reveal similar crystallographic orientation as that visible in shells from the 1970s and 2000s (Figures 2,3), with some evidence of shell fragility likely caused by ~ 1000 years spent in middens

shell means; TI: $t_{15} = 5.46$, $p < .001$, SP: $t_9 = 1.38$, $p = .198$), marking a temporal decline in Mg-O bond strength (Figure 5a). Mean Raman shift increased at Tatoosh from 1086.75 to 1086.89 cm^{-1} , indicating increasing Mg concentration, but declined at Sand Point from 1086.85 to 1086.72 cm^{-1} , indicating a decline in Mg concentration (t -test on shell means; TI: $t_{16} = 5.67$, $p < .001$, SP: $t_9 = -3.02$, $p = .014$; Figure 5a). Archival (1970s) and modern (1990s, 2000s, 2010s) samples did not differ in FWHM (t -test on shell means; archival mean 4.55, modern mean 4.61 cm^{-1} ; TI: $t_{16} = 0.899$, $p = .383$) or in Raman shift (t -test on shell means; archival mean 1086.87, modern mean 1086.89 cm^{-1} ; TI: $t_{17} = 0.850$, $p = .407$). Raman shift increased with ontogeny within each shell at both sites (linear mixed-effects model with individual shell as a random effect, individual age as a fixed effect; TI: coeff. = 0.0064, $p < .001$, number of meas. = 615, number of shells = 27; SP: coeff. = 0.0156, $p < .001$, number of meas. = 174, number of shells = 18; Figures S8, S9) but FWHM showed no significant ontogenetic trend (linear mixed-effects model with individual shell as a random effect, individual age as a fixed effect; TI: coeff. = 0.0019, $p = .426$, number of meas. = 615, number of shells = 27; SP: coeff. = 0.0055, $p = .251$, number of meas. = 174, number of shells = 18; Figures S8, S9).

3.3 | Increased variability in shell structure over time

Overall, variance in both bond strength and Mg content between individuals increased in modern samples. Standard deviation (SD) in FWHM increased from 0.19 to 0.35 (34%) at Sand Point ($F_{6,14} = 32.3$, $p = .004$) but did not show a significant change at Tatoosh Island, despite a 25% increase from 0.24 to 0.30 ($F_{6,14} = 2.82$, $p = .210$). Standard deviation (SD) in Raman shift increased from 0.112 to 0.162 (144%) at Tatoosh Island ($F_{6,14} = 32.3$, $p = .004$) and from 0.058 to 0.281 (484%) at Sand Point ($F_{7,9} = 38.4$, $p < .001$) between midden and modern shells (Figure 5b). The increased variability in *M. californianus* Mg-O bond strength is not fully explained by the variability in Mg content (Figure 5b; linear model $r^2 = .72$, $p = .068$).

4 | DISCUSSION

Measures of qualitative and quantitative shell traits over multiple adult individuals at two nearby sites allow for the robust detection of trends over time in a natural system and for measurement of

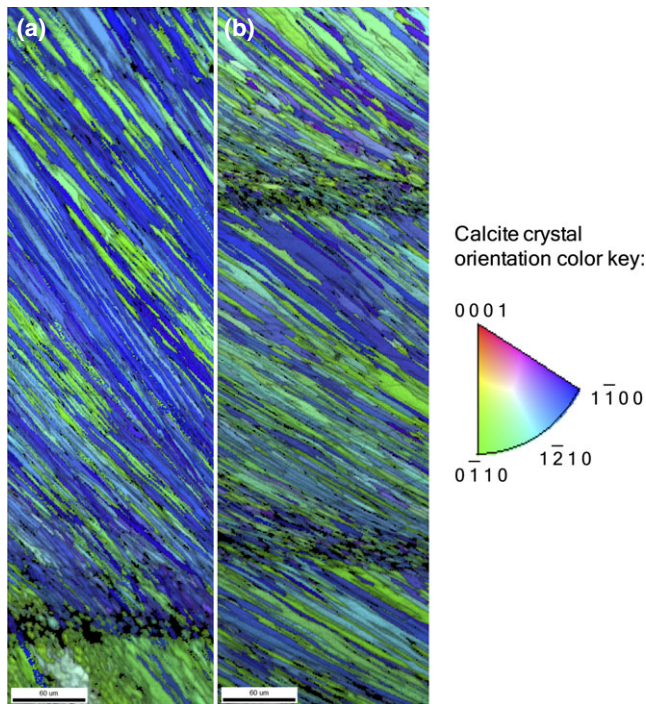


FIGURE 2 Electron backscatter diffraction (EBSD) analysis of archival shells collected 1975 (visible growth band ~1970) showing calcite crystallographic orientation map in reference to the {0001} plane, according to color key. Electron backscatter diffraction (EBSD) scans centered on a summer growth band from the center of the shell record (middle-age of individual), with most recent shell material at the bottom. Winter bands identified by horizontal bands of condensed crystal sizes and higher relative concentration of organic matter, revealed by black areas in the absence of crystal backscatter. (a) Shell TS10002, scale bar 60 μm ; (b) Shell TS10004, scale bar 60 μm . Refer to Figure S2 for an illustration of crystal orientation. These scans and those from modern 2000s shells (Figure 3) provide reference for typical shell crystallographic orientation in biogenic calcite

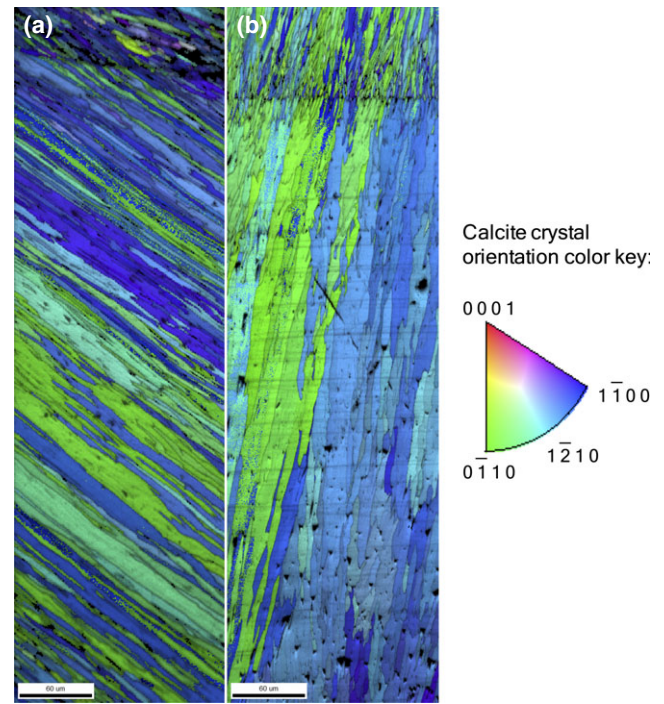


FIGURE 3 Electron backscatter diffraction (EBSD) analysis of modern 2000s shells collected 2009 (visible growth band ~2004) showing calcite crystallographic orientation map in reference to the {0001} plane, according to color key. Electron backscatter diffraction (EBSD) scans centered on a summer growth band from the center of the shell record (middle-age of individual), with most recent shell material at the bottom. Winter bands identified by horizontal bands of condensed crystal sizes and higher relative concentration of organic matter, revealed by black areas in the absence of crystal backscatter. (a) Shell GLO9002, scale bar 60 μm ; (b) Shell HCO9006, scale bar 60 μm . Refer to Figure S2 for an illustration of crystal orientation. Figure S5 shows a full transect of Shell HCO9006. These scans and those from archival 1970s shells (Figure 2) provide reference for typical shell crystallographic orientation in biogenic calcite

interindividual variability in those traits. Increased trait variability corresponds to an expectation of greater phenotypic plasticity under increased environmental stress. Trait values, including shell mineralogy, lead to fitness trade-offs (i.e. metabolic energy used to biomineralize, shell thickness to withstand predation or disturbance, growth rates), which may lead to selection for plastic developmental traits in unpredictable environments (Stearns, 1989). Similarly, stressful environments can select for genotypes that produce adaptive, reversible, plastic phenotypes (Gabriel, 2005).

Mg-O bond strength variability typically indicates increased positional disorder, or rotation of the CO_3^{2-} molecule out of the basal plane (Bischoff et al., 1985). This substantial increase in variability in Mg-O and Mg content in modern samples is also reflected in the significant, yet irregular, trends we observe in both metrics, and likely drives the inconsistency in directional change over time. This interpretation is compatible with our EBSD data, which shows increased variability in the orientation of CaCO_3 crystal units (changes in color, Figures 1–4) and decreased crystal size.

Our EBSD data for *M. californianus* are consistent with observations in *Mytilus edulis* (Fitzer et al., 2016), which also displayed reduced control over crystallographic orientation of calcite under experimental ocean acidification of 1000 μatm $p\text{CO}_2$, similar to acidification conditions reported in the present day at Tatoosh Island (Wootton & Pfister, 2012) and in other coastal systems (Hofmann et al., 2011; Wahl et al., 2015). In *M. edulis*, increased crystallographic variability has been attributed to an increase in amorphous calcium carbonate in both aragonitic and calcitic crystal phases (Fitzer et al., 2016). Raman data, however, suggest that *M. californianus* predominantly continues to precipitate calcite crystals. Electron backscatter diffraction (EBSD) scans show that those crystals become increasingly disorganized and fine-grained in our most recent 2015 samples.

This decadal and centennial time series of shells enabled us to study population-scale responses to 'natural' acidification over time. Yet, the rapid onset of the severity of recent pH excursions suggested by $\delta^{13}\text{C}$ concentrations from these same shells (Pfister et al.,

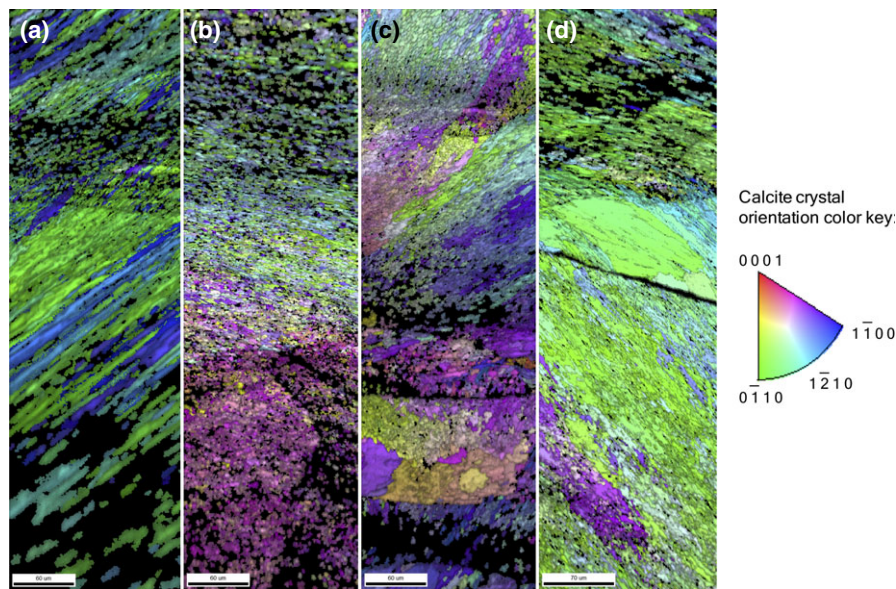


FIGURE 4 Electron backscatter diffraction (EBSD) analysis of modern 2010s shells collected 2015 (visible growth band ~2012) showing calcite crystallographic orientation map in reference to the {0001} plane, according to color key. Electron backscatter diffraction (EBSD) scans centered on a summer growth band from the center of the shell record (middle-age of individual), with most recent shell material at the bottom. Winter bands identified by horizontal bands of condensed crystal sizes and higher relative concentration of organic matter, revealed by black areas in the absence of crystal backscatter. (a) Shell GL15007, scale bar 60 μm ; (b) Shell GL15005, scale bar 60 μm ; (c) Shell HC15003, scale bar 60 μm ; and (d) Shell HC15004, scale bar 70 μm . Refer to Figure S6 for additional images and to Figure S2 for an illustration of crystal orientation. These shells show distinct areas of amorphous calcium carbonate, particularly in panels (b) and (c), and suggest variability between individuals

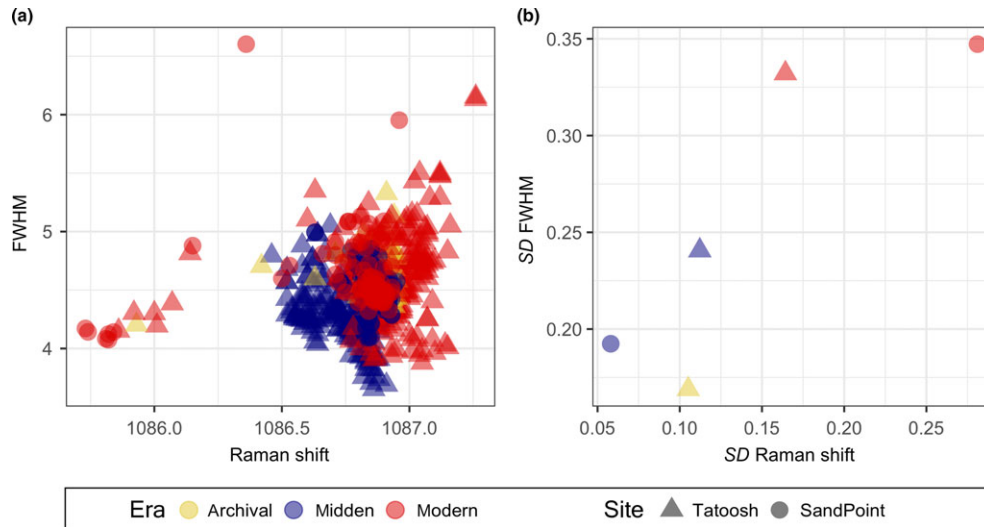


FIGURE 5 (a) Raman peak full width at half peak maximum (FWHM), indicating Mg-O bond strength, and Raman shift (cm^{-1}), indicating Mg content. (b) Standard deviations plotted by site and era. Overlapping points appear more vivid

2011) relative to the length of our record suggests that adaptation or acclimatization in subsequent generations to these most recent changes may still be forthcoming. Our study used only adult *M. californianus*, a long-lived species relative to its congeners. It is noteworthy that *M. edulis* juveniles spawned from parents living in experimental acidified conditions grew shells containing only calcite, in contrast to the bimineralic (aragonitic and calcitic) shells of their parents (Fitzer et al., 2014).

Other, aragonite-containing *Mytilus* species have shown a diversity of responses to changes in seawater carbonate chemistry, including decreased size and shell thickness during larval stages, decreases in shell density, shell dissolution, and weakened byssal threads (Fitzer et al., 2014, 2015, 2016; Gaylord et al., 2011; O'Donnell, George, & Carrington, 2013; Thomsen et al., 2010). *Mytilus californianus* shell mineralogy should be more resistant to ocean acidification compared with other bivalves because it is the only

mussel to lay down calcite instead of aragonite in its inner shell layer (Dodd, 1964), which is exposed to ambient seawater when mussels are feeding at high tide. This trait may explain its ability to continue biomineralizing under reduced pH conditions.

Because *M. californianus* is almost exclusively found in the already-acidic California current system, its inner prismatic calcite layer may represent a plastic or evolutionary response to long-term acidification stress in this region, over hundreds or possibly thousands of years. Electron backscatter diffraction (EBSD) scans spanning all growth layers of midden shells indicate that *M. californianus* has grown a calcitic inner prismatic layer for at least 1000 years. However, the inner prismatic calcite layer in *M. californianus* has thinned by half (Pfister et al., 2016), despite changing seawater carbon chemistry over the same interval (Pfister et al., 2011). Thus, the number of deleterious effects of ocean acidification demonstrated for *M. californianus* suggests that it is still vulnerable to ocean acidification effects, including ad-hoc biomineralization as acidification continues. Together with possible niche constriction as its upper elevational limit becomes restricted by increasing temperatures (Harley, 2011), this forms an alarming prognosis for the future of *M. californianus*, a foundational species that supports hundreds of associated organisms in its bed structure (Suchanek, 1992).

Our results reveal increased disorder in the calcium carbonate shells of the California mussel, *M. californianus*, as a result of increased acidification. Shell mineralogy has altered dramatically over the past 15 years, despite evidence for 2500 years of consistent mineral structure in the calcitic inner prismatic layer. Increased shell structure variability, in particular, has emerged as a primary response to acidification stress in shell formation in adult *M. californianus*, despite an expectation of increased resistance to acidification based on the shell mineralogy of this *Mytilus* species. Increased variability is a theme that has emerged over terrestrial and marine climate change responses at the broadest scale (CaraDonna, Iler, & Inouye, 2014; Inouye, 2008; Kroeker et al., 2010; Ovaskainen & Skorokhodova, 2013), reflecting differential fragilities and trade-offs that may affect survival between genotypes, populations, or microhabitats. While increases in variability reveal the vulnerability of organisms to environmental changes, they may also indicate potential for resilience or recovery.

ACKNOWLEDGEMENTS

We thank the Makah Tribal Nation for access to Tatoosh Island and midden shells, with special thanks to J. Ledford, G. Wessen, and the Makah Cultural and Research Center. The Olympic National Park loaned Sand Point material (Permit OLYM-2010-CI-0056), with thanks to D. Conca and G. Hunter. A. Barner, B. Coulson, and J. Gilleece provided assistance with shell sectioning and polishing. SJM and NAK are grateful for a Marine Alliance for Science and Technology Scotland (MASTS) Postdoctoral and Early Career Research Exchange, which provided funding for this work. SJM was supported by a Marie Curie International Incoming Fellowship within the 7th European Community Framework Programme (grant agreement

FP7-PEOPLE-2012-IIF No. 330271). Funding to obtain and radiocarbon date shells was provided by the SeaDoc Society (CAP), NSF grants OCE01-17801 (JTW and CAP), OCE09-28232 (CAP), DEB09-19420 and DEB15-56874 (JTW).

CONFLICT OF INTEREST

The authors declare no conflict of interest.

ORCID

Sophie J. McCoy  <http://orcid.org/0000-0003-1324-1578>

Nicholas A. Kamenos  <http://orcid.org/0000-0003-3434-0807>

Timothy J. Wootton  <http://orcid.org/0000-0002-7715-0344>

Catherine A. Pfister  <http://orcid.org/0000-0003-0892-637X>

REFERENCES

- Bischoff, W. D., Sharma, S. K., & MacKenzie, F. T. (1985). Carbonate ion disorder in synthetic and biogenic magnesian calcites: A Raman spectral study. *American Mineralogist*, 70, 581–589.
- CaraDonna, P. J., Iler, A. M., & Inouye, D. W. (2014). Shifts in flowering phenology reshape a subalpine plant community. *Proceedings of the National Academy of Sciences of the United States of America*, 111, 4916–4921. <https://doi.org/10.1073/pnas.1323073111>
- Chan, F., Barth, J. A., Blanchette, C. A., Byrne, R. H., Chavez, F., Cheriton, O., ... Washburn, L. (2017). Persistent spatial structuring of coastal ocean acidification in the California current system. *Scientific Reports*, 7, 255–257.
- Cobb, K. M., Charles, C. D., Cheng, H., & Edwards, R. L. (2003). El Niño/Southern Oscillation and tropical Pacific climate during the last millennium. *Nature*, 424, 271–276. <https://doi.org/10.1038/nature01779>
- Coe, W. R. (1945). Nutrition and growth of the California Bay-mussel (*Mytilus edulis diegensis*). *Journal of Experimental Zoology*, 99, 1–14. [https://doi.org/10.1002/\(ISSN\)1097-010X](https://doi.org/10.1002/(ISSN)1097-010X)
- Cooley, S. R., & Doney, S. C. (2009). Anticipating ocean acidification's economic consequences for commercial fisheries. *Environmental Research Letters*, 4, 024007. <https://doi.org/10.1088/1748-9326/4/2/024007>
- Dodd, J. R. (1964). Environmentally controlled variation in the shell structure of a pelecypod species. *Journal of Paleontology*, 38, 1065–1071.
- Feely, R. A., Sabine, C. L., Byrne, R. H., Millero, F. J., Dickson, A. G., Wanninkhof, R., ... Greeley, D. (2012). Decadal changes in the aragonite and calcite saturation state of the Pacific Ocean. *Global Biogeochemical Cycles*, 26, GB3001.
- Feely, R. A., Sabine, C. L., Hernandez-Ayon, J. M., Ianson, D., & Hales, B. (2008). Evidence for upwelling of corrosive "acidified" water onto the continental shelf. *Science*, 320, 1490–1492. <http://doi.org/10.1126/science.1155676>
- Fitzer, S. C., Chung, P., Maccherozzi, F., Dhesi, S. S., Kamenos, N. A., Phoenix, V. R., & Cusack, M. (2016). Biomineral shell formation under ocean acidification: A shift from order to chaos. *Scientific Reports*, 6, 21076. <https://doi.org/10.1038/srep21076>
- Fitzer, S. C., Cusack, M., Phoenix, V. R., & Kamenos, N. A. (2014). Ocean acidification reduces the crystallographic control in juvenile mussel shells. *Journal of Structural Biology*, 188, 39–45. <http://doi.org/10.1016/j.jsb.2014.08.007>
- Fitzer, S. C., Vittert, L., Bowman, A., Kamenos, N. A., Phoenix, V. R., & Cusack, M. (2015). Ocean acidification and temperature increase impact mussel shell shape and thickness: Problematic for protection? *Ecology and Evolution*, 5, 4875–4884. <https://doi.org/10.1002/ece3.1756>

- Fox, D. L., & Coe, W. R. (1943). Biology of the California sea-mussel (*Mytilus californianus*). II. Nutrition, metabolism, growth and calcium deposition. *Journal of Experimental Biology*, 205, 205–249.
- Gabriel, W. (2005). How stress selects for reversible phenotypic plasticity. *Journal of Evolutionary Biology*, 18, 873–883. <https://doi.org/10.1111/j.1420-9101.2005.00959.x>
- Gaylord, B., Hill, T. M., Sanford, E., Lenz, E. A., Jacobs, L. A., Sato, K. N., ... Hettlinger, A. (2011). Functional impacts of ocean acidification in an ecologically critical foundation species. *Journal of Experimental Biology*, 214, 2586–2594. <https://doi.org/10.1242/jeb.055939>
- Gazeau, F., Parker, L. M., Comeau, S., Gattuso, J.-P., O'Connor, W. A., Martin, S., ... Ross, P. M. (2013). Impacts of ocean acidification on marine shelled molluscs. *Marine Biology*, 160, 2207–2245. <https://doi.org/10.1007/s00227-013-2219-3>
- Gooding, R. A., Harley, C. D. G., & Tang, E. (2009). Elevated water temperature and carbon dioxide concentration increase the growth of a keystone echinoderm. *Proceedings of the National Academy of Sciences*, 106, 9316–9321. <https://doi.org/10.1073/pnas.0811143106>
- Hahn, S., Rodolfo-Metalpa, R., Griesshaber, E., Schmahl, W. W., Buhl, D., Hall-Spencer, J. M., ... Immenhauser, A. (2011). Marine bivalve geochemistry and shell ultrastructure from modern low pH environments. *Biogeosciences Discussions*, 8, 10351–10388. <https://doi.org/10.5194/bgd-8-10351-2011>
- Halfar, J., Adey, W. H., & Kronz, A. (2013). Arctic sea-ice decline archived by multicentury annual-resolution record from crustose coralline algal proxy. *Proceedings of the National Academy of Sciences of the United States of America*, 110(49), 19737–19741. <https://doi.org/10.1073/pnas.1313775110>
- Hall-Spencer, J. M., Rodolfo-Metalpa, R., Martin, S., Ransome, E., Fine, M., Turner, S. M., ... Buia, M. C. (2008). Volcanic carbon dioxide vents show ecosystem effects of ocean acidification. *Nature*, 454, 96–99. <https://doi.org/10.1038/nature07051>
- Harley, C. D. G. (2011). Climate change, keystone predation, and biodiversity loss. *Science*, 334, 1124–1127. <https://doi.org/10.1126/science.1210199>
- Hofmann, G. E., Barry, J. P., Edmunds, P. J., Gates, R. D., Hutchins, D. A., Klinger, T., & Sewell, M. A. (2010). The effect of ocean acidification on calcifying organisms in marine ecosystems: An organism-to-ecosystem perspective. *Annual Review of Ecology, Evolution, and Systematics*, 41, 127–147. <https://doi.org/10.1146/annurev.ecolsys.110308.120227>
- Hofmann, G. E., Smith, J. E., Johnson, K. S., Send, U., Levin, L. A., Micheli, F., ... Martz, T. R. (2011). High-frequency dynamics of ocean pH: A multi-ecosystem comparison (ed Chin W-C). *PLoS ONE*, 6, e28983. <https://doi.org/10.1371/journal.pone.0028983>
- Inouye, D. W. (2008). Effects of climate change on phenology, frost damage, and floral abundance of montane wildflowers. *Ecology*, 89, 353–362. <https://doi.org/10.1890/06-2128.1>
- Jacob, D. E., Soldati, A. L., Wirth, R., Huth, J., Wehrmeister, U., & Hofmeister, W. (2008). Nanostructure, composition and mechanisms of bivalve shell growth. *Geochimica et Cosmochimica Acta*, 72, 5401–5415. <https://doi.org/10.1016/j.gca.2008.08.019>
- Kroeker, K. J., Kordas, R. L., Crim, R. N., & Singh, G. G. (2010). Meta-analysis reveals negative yet variable effects of ocean acidification on marine organisms. *Ecology Letters*, 13, 1419–1434. <https://doi.org/10.1111/j.1461-0248.2010.01518.x>
- Kroeker, K. J., Kordas, R. L., & Harley, C. D. G. (2017). Embracing interactions in ocean acidification research: Confronting multiple stressor scenarios and context dependence. *Biology Letters*, 13, 20160802–20160804. <https://doi.org/10.1098/rsbl.2016.0802>
- Kroeker, K. J., Sanford, E., Rose, J. M., Blanchette, C. A., Chan, F., Chavez, F. P., ... Russell, A. D. (2016). Interacting environmental mosaics drive geographic variation in mussel performance and predation vulnerability. *Ecology Letters*, 19, 771–779. <https://doi.org/10.1111/ele.12613>
- Leung, J. Y. S., Russell, B. D., & Connell, S. D. (2017). Mineralogical Plasticity Acts as a Compensatory Mechanism to the Impacts of Ocean Acidification. *Environmental Science & Technology*, 51, 2652–2659. <https://doi.org/10.1021/acs.est.6b04709>
- Mann, M. E., Zhang, Z., Hughes, M. K., Bradley, R. S., Miller, S. K., Rutherford, S., & Ni, F. (2008). Proxy-based reconstructions of hemispheric and global surface temperature variations over the past two millennia. *Proceedings of the National Academy of Sciences*, 105, 13252–13257. <https://doi.org/10.1073/pnas.0805721105>
- McCoy, S. J., & Pfister, C. A. (2014). Historical comparisons reveal altered competitive interactions in a guild of crustose coralline algae (ed Jackson S). *Ecology Letters*, 17, 475–483. <https://doi.org/10.1111/ele.12247>
- McCoy, S. J., & Ragazzola, F. (2014). Skeletal trade-offs in coralline algae in response to ocean acidification. *Nature Climate Change*, 4, 719–723. <https://doi.org/10.1038/nclimate2273>
- McMillan, A. D. (2000). *Since the time of the transformers: The ancient heritage of the Nuu-Chah-Nulth, Ditidaht, and Makah*. Vancouver, BC: UBC Press.
- Melzner, F., Stange, P., Trübenbach, K., Thomsen, J., Casties, I., Panknin, U., ... Gutowska, M. A. (2011). Food Supply and Seawater pCO₂ Impact Calcification and Internal Shell Dissolution in the Blue Mussel *Mytilus edulis*. *PLoS ONE*, 6, e24223. <https://doi.org/10.1371/journal.pone.0024223>
- Mount, A. S., Wheeler, A. P., Paradkar, R. P., & Snider, D. (2004). Hemocyte-mediated shell mineralization in the eastern oyster. *Science*, 304, 297–300. <https://doi.org/10.1126/science.1090506>
- Nash, M. C., Opdyke, B. N., Troitzsch, U., Russell, B. D., Adey, W. H., Kato, A., ... Kline, D. I. (2012). Dolomite-rich coralline algae in reefs resist dissolution in acidified conditions. *Nature Climate Change*, 2, 1–5.
- O'Donnell, M. J., George, M. N., & Carrington, E. (2013). Mussel byssus attachment weakened by ocean acidification. *Nature Climate Change*, 18, 587–590. <http://doi.org/10.1038/NCLIMATE1846>
- Orr, J. C., Fabry, V. J., Aumont, O., Bopp, L., Doney, S. C., Feely, R. A., ... Yool, A. (2005). Anthropogenic ocean acidification over the twenty-first century and its impact on calcifying organisms. *Nature*, 437, 681–686. <https://doi.org/10.1038/nature04095>
- Ovaskainen, O., & Skorokhodova, S. (2013). Community-level phenological response to climate change. *Proceedings of the National Academy of Sciences*, 110, 13434–13439. <https://doi.org/10.1073/pnas.1305533110>
- Palmer, A. R. (1983). Relative cost of producing skeletal organic matrix versus calcification: Evidence from marine gastropods. *Marine Biology*, 75, 287–292. <https://doi.org/10.1007/BF00406014>
- Pauly, M., Kamenos, N. A., Donohue, P., & LeDrew, E. (2015). Coralline algal Mg-O bond strength as a marine pCO₂ proxy. *Geology*, 43, 267–270. <https://doi.org/10.1130/G36386.1>
- Pérez-Huerta, A., Cusack, M., McDonald, S., Marone, F., Stampanoni, M., & MacKay, S. (2009). Brachiopod punctae: A complexity in shell biomineralisation. *Journal of Structural Biology*, 167, 62–67. <https://doi.org/10.1016/j.jsb.2009.03.013>
- Pfister, C. A., McCoy, S. J., Wootton, J. T., Martin, P. A., Colman, A. S., & Archer, D. (2011). Rapid environmental change over the past decade revealed by isotopic analysis of the California Mussel in the Northeast Pacific. *PLoS ONE*, 6, e25766. <https://doi.org/10.1371/journal.pone.0025766>
- Pfister, C. A., Roy, K., Wootton, J. T., McCoy, S. J., Paine, R. T., Suchanek, T. H., & Sanford, E. (2016). Historical baselines and the future of shell calcification for a foundation species in a changing ocean. *Proceedings of the Royal Society B: Biological Sciences*, 283, 20160392–20160398. <https://doi.org/10.1098/rspb.2016.0392>
- Ries, J. B. (2005). Aragonite production in calcite seas: Effect of seawater Mg/Ca ratio on the calcification and growth of the calcareous alga

- Penicillus capitatus*. *Paleobiology*, 31, 445–458. [https://doi.org/10.1666/0094-8373\(2005\)031\[0445:APICSE\]2.0.CO;2](https://doi.org/10.1666/0094-8373(2005)031[0445:APICSE]2.0.CO;2)
- Ries, J. B., Anderson, M. A., & Hill, R. T. (2008). Seawater Mg/Ca controls polymorph mineralogy of microbial CaCO₃: A potential proxy for calcite-aragonite seas in Precambrian time. *Geobiology*, 6, 106–119. <https://doi.org/10.1111/j.1472-4669.2007.00134.x>
- Stearns, S. C. (1989). The evolutionary significance of phenotypic plasticity. *BioScience*, 39, 436–445. <https://doi.org/10.2307/1311135>
- Stumpp, M., Wren, J., Melzner, F., Thorndyke, M. C., & Dupont, S. T. (2011). CO₂ induced seawater acidification impacts sea urchin larval development I: Elevated metabolic rates decrease scope for growth and induce developmental delay. *Comparative Biochemistry and Physiology, Part A*, 160, 331–340. <https://doi.org/10.1016/j.cbpa.2011.06.022>
- Suchanek, T. H. (1992). Extreme biodiversity in the marine environment - Mussel bed communities of *Mytilus californianus*. *Northwest Environmental Journal*, 8, 150–152.
- Thomsen, J., Gutowska, M. A., Saphörster, J., Heinemann, A., Trübenbach, K., Fietzke, J., ... Melzner, F. (2010). Calcifying invertebrates succeed in a naturally CO₂-rich coastal habitat but are threatened by high levels of future acidification. *Biogeosciences*, 7, 3879–3891. <https://doi.org/10.5194/bg-7-3879-2010>
- Thomsen, J., Haynert, K., Wegner, K. M., & Melzner, F. (2015). Impact of seawater carbonate chemistry on the calcification of marine bivalves. *Biogeosciences*, 12, 4209–4220. <https://doi.org/10.5194/bg-12-4209-2015>
- Thomsen, J., & Melzner, F. (2010). Moderate seawater acidification does not elicit long-term metabolic depression in the blue mussel *Mytilus edulis*. *Marine Biology*, 157, 2667–2676. <https://doi.org/10.1007/s00227-010-1527-0>
- Vermeij, G. J. (1976). Interoceanic differences in vulnerability of shelled prey to crab predation. *Nature*, 260, 135–136. <https://doi.org/10.1038/260135a0>
- Wahl, M., Buchholz, B., Winde, V., Golomb, D., Guy-Haim, T., Muller, J., ... Bottcher, M. E. (2015). A mesocosm concept for the simulation of near-natural shallow underwater climates: The Kiel Outdoor Benthocosms (KOB). *Limnology and Oceanography: Methods*, 13, 651–663. <https://doi.org/10.1002/lom3.10055>
- Waldbusser, G. G., Brunner, E. L., Haley, B. A., Hales, B., Langdon, C. J., & Prah, F. G. (2013). A developmental and energetic basis linking larval oyster shell formation to acidification sensitivity. *Geophysical Research Letters*, 40, 2171–2176. <https://doi.org/10.1002/grl.50449>
- Weiner, S., & Addadi, L. (2011). Crystallization pathways in biomineralization. *Annual Review of Materials Research*, 41, 21–40. <https://doi.org/10.1146/annurev-matsci-062910-095803>
- Weiss, I. M., Tuross, N., Addadi, L., & Weiner, S. (2002). Mollusc larval shell formation: Amorphous calcium carbonate is a precursor phase for aragonite. *Journal of Experimental Zoology*, 293, 478–491. [https://doi.org/10.1002/\(ISSN\)1097-010X](https://doi.org/10.1002/(ISSN)1097-010X)
- Wootton, J. T., & Pfister, C. A. (2012). Carbon system measurements and potential climatic drivers at a site of rapidly declining ocean pH (ed Chin W-C). *PLoS ONE*, 7, e53396. <https://doi.org/10.1371/journal.pone.0053396>
- Wootton, J. T., Pfister, C. A., & Forester, J. D. (2008). Dynamic patterns and ecological impacts of declining ocean pH in a high-resolution multi-year dataset. *Proceedings of the National Academy of Sciences*, 105, 18848–18853. <https://doi.org/10.1073/pnas.0810079105>

SUPPORTING INFORMATION

Additional Supporting Information may be found online in the supporting information tab for this article.

How to cite this article: McCoy SJ, Kamenos NA, Chung P, Wootton JT, Pfister CA. A mineralogical record of ocean change: Decadal and centennial patterns in the California mussel. *Glob Change Biol*. 2017;00:1–9. <https://doi.org/10.1111/gcb.14013>